

# Investigation of Finned heat pipe on compact heat exchanger in waste heat recovery application – Experimental analysis

Ramkumar P<sup>1\*</sup>, Thilagapathy G<sup>1</sup>, Thinagar A<sup>1</sup>, Chendur M<sup>1</sup>, Loga Rajakumari B<sup>1</sup>, Mothibala S<sup>1</sup>

<sup>1</sup> Department of Aeronautical Engineering, Kalasalingam Academy of Research and Education, Krishnankoil, Tamilnadu 626126, India.

**Abstract.** Heat exchangers are essential components in a wide range of industrial processes by enabling efficient thermal energy transfer among fluids, significantly impacting overall system performance. This study examines the effective heat transfer of a concentric tube heat exchanger enhanced with finned heat pipes, aiming to optimize heat energy recovery and improve energy efficiency. Experimental investigations are conducted under varying inlet temperatures (70°C to 90°C) and fluid flow rates (0.0138 to 0.0555 kg/s) to evaluate key performance metrics, including heat transfer rates, heat transfer coefficients, and system effectiveness. Results reveal that higher inlet temperatures and mass flow rates significantly boost thermal performance, achieving a maximum heat transfer coefficient of 2211.91 W/m<sup>2</sup>°C and effectiveness of 39.1% at 90°C and 0.0555 kg/s, similarly the observed Reynolds number for this condition is 2771 this shows flow is laminar and resulting in uniform heat transfer within the heat exchanger. The integration of finned heat pipes enhances maximum contact surface area and thermal gradients with flowing fluids and heat pipe, thus enabling superior energy recovery compared to conventional systems. These findings underscore the potential of finned heat pipe technology for sustainable and efficient thermal management solutions in industrial waste heat recovery systems to enhance the affordable clean energy and minimize the climate action.

---

\*Corresponding author: [rkmailmech@gmail.com](mailto:rkmailmech@gmail.com)

## 1 Introduction

Heat exchangers are used for decades in numerous industrial sectors to ensure the effective heat transfer across fluids or between a fluid and a solid surface without mixing the fluids or physical contact. Their role in optimizing energy use, enhancing system performance, and maintaining desired operational temperatures underscores their importance in applications ranging from power generation to automotive engineering. Among the various designs, the incorporation of finned heat pipes within heat exchangers has emerged as a significant innovation for improving thermal performance, compactness, and energy efficiency. The high integral fins improve heat transfer by expanding surface contact for significant heat energy transfer, it is crucial in efficient heat management along systems like HVAC and power plants. Their use of mathematical modelling and computational fluid dynamics (CFD) further validates experimental data and assists in optimizing design parameters, such as fin height and spacing, for improved performance. This combined approach provides insights into creating more efficient and thermally effective finned tube heat exchangers [1]. The importance of fin geometry in enhancing thermal performance. Literature suggests that increasing surface area and inducing turbulence through high integral fins significantly improve heat transfer efficiency, particularly in compact heat exchangers used in HVAC, automotive, and energy production. Combining experimental results with theoretical models helps refine the design of these heat exchangers for better performance under varying conditions [2]. An improving automotive thermoelectric generator (ATEGs) by integrating heat pipes within the heat exchanger design. This enhancement expands the hot-side surface area, leading to a 42.95% boost in output power and a 55.6% increase in heat absorption. Numerical models optimize heat pipe configuration, significantly improving energy recovery and generator efficiency [3]. The transient thermal efficiency in micro heat pipes, focusing on heat transfer characteristics and their response under varying thermal loads. Their insights demonstrate the efficiency and reliability of micro heat pipes in thermal management applications [4]. Thermal performance and environmental impact of alternative working fluids. The study identifies sustainable options for heat transfer systems by investigating low global warming potential (GWP) fluids [5]. Efficiency on closed loop pulsating heat pipe with different gravitational effect provide valuable data on the thermal performance of heat pipes in different gravitational situations. This research is especially relevant for space applications, where gravitational variations impact heat pipe performance [6]. The thermal performance and flow behavior in minimum condenser diameter of Loop Heat Pipes (LHP) and Capillary Pumped Loops (CPL) enhances the heat transfer mechanisms through experimental findings [7]. The design and performance improvements needed to enhance the operational range of LHP for various applications [8]. The behavior of the three contact line on a heater associated with non-isothermal limited moistening is analyzed. It offers a theoretical model to describe the behavior of the contact line, which is essential for predicting heat transfer rates in heat pipes [9]. Investigation on Pulsating Heat Pipe (PHP) along dynamic film model shows significant importance of dynamic film and its performance enhancement in PHP [10]. The investigation are done on LHP using transient thermo-fluid modelling using various operating conditions shows significant improvement in the system [11]. Analysis are carried out on Micro-Flat Heat Pipe (MFHP) with three dimension integrated compact cooling system to enhance the thermal management. This shows significant in design and performance benefits on efficient cooling in compact electronic devices [12]. The experimental and numerical approached on the impact of triple phase contact line enhances the evaporative heat transfer on denoting the speed and significant improvement on optimizing the HP performance [13]. The literature shows the

utilization of finned heat pipe is limited for the investigation with minimum parameters. This study focuses on the T-Shaped heat pipe with fin configuration using DI water as heat transfer medium. The observations focused on heat transfer rate, Effectiveness of the system and influence of fin configurations in heat transfer performance and this system demonstrates potential as a highly efficient waste heat recovery solutions.

## 2 Experimental fabrication and procedure

### 2.1 Fabrication of test model

The three copper pipes are used for fabricating the Heat Pipes (HP) with a length of 220 millimetres and a diameter of 12 millimetres. This heat pipe is kept vertically with the dimensions of 100 millimetres as evaporator, 70 millimetres as condenser and 50 millimetres as adiabatic sections, respectively. The circular copper fins of 60 millimetres are attached at the condenser zone of the HP to enhance the maximum surface area contact with the liquid and heat pipe.

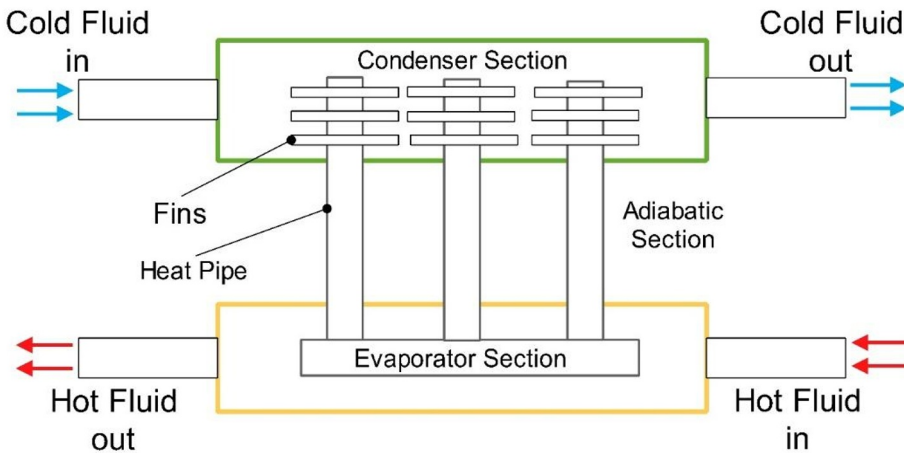


**Fig 1.** Schematic model of FHPHE

The stainless steel wire mesh of 50 holes per inch and wire diameter of  $0.2 \times 10^{-3}$  m is used as wick for the heat pipe. The schematic diagram of Finned Heat Pipe Heat Exchanger (FHPHE) is shown as Figure 1. Di-ionised (DI) water working fluid is used to carry the heat in the heat pipe, having 75% fill ratio this measures volume rate of 55 millilitres of evaporator section. Galvanized iron is used to construct the structure of the heat exchanger, which measures 270 millimetres in length and 70 millimetres in diameter. The different sectional view of FHPHE is given in Figure 2 (a), (b), (c). The outer structure of heat exchanger is insulated with 10 millimetres styrofoam material for preventing the dissipation of heat over the environment.

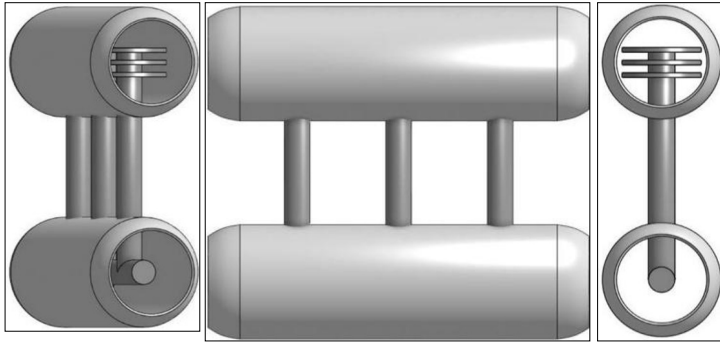


**Fig 2.** (a), (b), (c) Sectional views of FHPHE

## 2.2 Experimentation Procedure

The T shaped cylindrical copper pipe is used for fabricating the HP is shown in Figure 3 (a), the vertical portion is placed at condenser section and similarly horizontal portion is placed at evaporator section of heat exchanger as Figure 3(b).

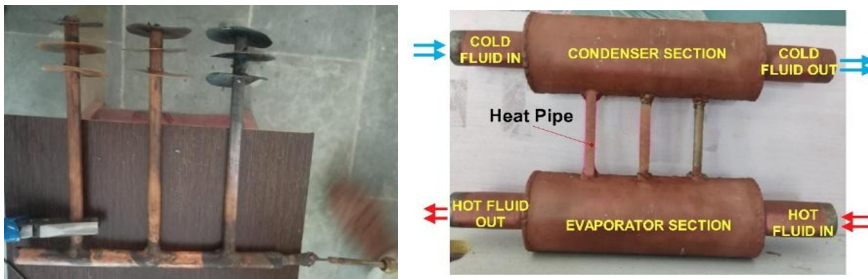


**Fig 3.** (a), (b). Fabricated finned heat pipe heat exchanger test model

The circular copper fins are fabricated and placed at the condenser portion in HP, this improves the area of surface contact for enhancing the heat interaction. The experimentation is carried out with the various input parameters such as the mass flow rates of hot water ( $m_{hi}$ ) are set to be ranging from 0.0138, 0.0277, 0.0416 and 0.0555 Kg/s. Similarly the cold water mass flow rate ( $m_{ci}$ ) is ranging from 0.069, 0.0139, 0.0208 and 0.0278 Kg/s, and the flow rates are measured and controlled by the rotameters. The inlet temperatures of hot water ( $T_{hi}$ ) are 70°C, 75°C, 80°C, 85°C and 90°C inlet temperature of cold water ( $T_{ci}$ ) is set as ambient temperature which is 33 °C. The DI water physical properties [14] are given in Table 1. The thermometry of the all junctions and surface of HP are done using the K-type thermocouple in the FHPHE. The experimentation is conducted with fabricated FHPHE, the hot fluid is pumped from hot water tank of 3 litres capacity with 1 HP pump. The pumped hot water is measured and controlled using rotameter, the measured flow rates are enters into the hot fluid inlet section of the heat exchanger, where the heat present in the hot fluid is transferred to the DI water working fluid in the HP thus liquid DI water is converted into vapour and formed vapour moves towards the adiabatic section, here no heat interaction takes place into the system and thus formed vapour moves towards condenser section. The cold fluid is pumped



The initial experimentation is conducted for  $T_{hi}$  of  $70^{\circ}\text{C}$  and  $m_{hi}$  of  $0.0138\text{ Kg/s}$  and similarly for  $T_{ci}$  is maintained at  $33^{\circ}\text{C}$  (ambient condition) throughout the experimentation and  $m_{ci}$  as  $0.069\text{ Kg/s}$ . The similar experimentation is conducted with different input temperatures such as  $75^{\circ}\text{C}$ ,  $80^{\circ}\text{C}$ ,  $85^{\circ}\text{C}$  and  $90^{\circ}\text{C}$ , with different  $m_{hi}$  as  $0.0277$ ,  $0.04160$  and  $0.0556\text{ Kg/s}$ , with various  $m_{ci}$  as  $0.0139$ ,  $0.0208$  and  $0.0278\text{ Kg/s}$ , respectively. This experimentation is conducted at regular time interval by attaining the steady state condition, it's observed that each cycle run time for each set of reading as 15 minutes. The DI water working fluid used for the experimentation, the different heat input temperatures makes the working fluid encounters the phase change in both the sections due to the capillary action of the wick this makes the continuous heat transfer in the HP. The experimentation process is given in the Figure 4, the hot and cold fluid circulation are shown using red and blue lines.  $T_c$ ,  $T_{ci}$ ,  $T_{co}$ ,  $T_h$ ,  $T_{hi}$ ,  $T_{ho}$  are cold and hot fluid inlet and out temperatures, respectively.  $T_{c1}$  and  $T_{e1}$  are the evaporator and condenser zones surface temperatures.  $TSHP1$ ,  $TSHP2$ ,  $TSHP3$ , are the HP's surface temperature.  $TVHP$  as evaporator portion temperature of the heat pipe. The thermocouples are connected in all the node to monitor the temperature of the FHPHE and it's shown in temperature indicator it is mounted in the control panel. The Figure 5, shows the image of the experimental model.

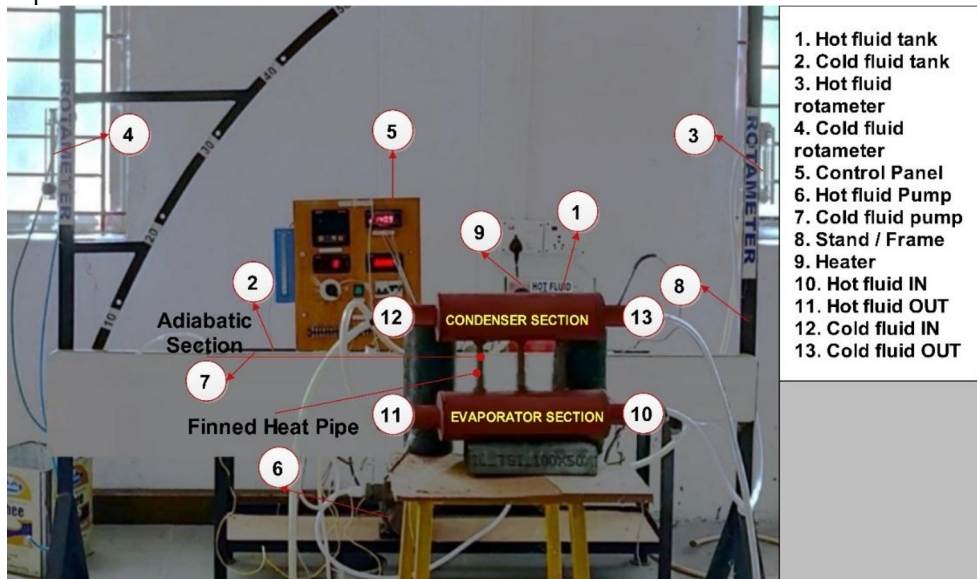


Fig 5. Photographic view of the FHPHE

### 2.3 Experimental Uncertainty

The uncertainty of the FHPHE experimentation is calculated using the Kline and McClintock method proposed by J. P. Holman [15] is given in below equations (10 – 13) for different parameters such as Heat transfer coefficient ( $h$ ), Effectiveness ( $E$ ), Reynolds ( $Re$ ) and Heat transfer rate ( $Q$ ).

The experiments are conducted with different instruments and there instrumental uncertainty is stated for Rotameters as  $\pm 0.1\%$ , Ammeter denotes  $\pm 0.5\%$ , K type thermocouples shows

$\pm 0.2^\circ\text{C}$ , Voltmeter denotes  $\pm 0.5\%$ , and, respectively. The instrumental uncertainty is minimised using frequent calibration with national standards.

$$\frac{d\epsilon}{\epsilon} = \left[ \left( \frac{d\dot{m}}{\dot{m}} \right)^2 + \left( \frac{d\Delta T}{\Delta T} \right)^2 \right]^{0.5} \quad (10)$$

$$\frac{dh}{h} = \left[ \left( \frac{dQ}{Q} \right)^2 + \left( \frac{d\Delta T}{\Delta T} \right)^2 \right]^{0.5} \quad (11)$$

$$\frac{dQ}{Q} = \left[ \left( \frac{d\dot{m}}{\dot{m}} \right)^2 + \left( \frac{d\Delta T}{\Delta T} \right)^2 \right]^{0.5} \quad (12)$$

$$\frac{d(\text{Re})}{(\text{Re})} = \left[ \left( \frac{d\dot{m}}{\dot{m}} \right)^2 \right]^{0.5} \quad (13)$$

The experimental uncertainty measured for  $E$ ,  $h$ ,  $Q$ , and  $\text{Re}$  as 5.7%, 4.9%, 4.1%, and 5.4%, respectively.

### 3 Results and Discussion

The investigation is carried out with the finned cylindrical copper HP inserted in heat exchanger, the experimentation is done to analyse the performance of the FHPHE by utilizing the heat from the hot fluid as input heat with different temperatures such as  $70^\circ\text{C}$  to  $90^\circ\text{C}$  with  $5^\circ\text{C}$  increment, and with various mass flow rates are 0.0138, 0.0277, 0.0416 and 0.0555 Kg/s for the evaporator region and thus this source of heat vaporizes the liquid DI water and this vapour transfers the heat energy to the condenser region, this heat transforms the cold inlet liquid entering in this region to hot liquid. This procedure of heat transfer is analysed for different hot input temperatures and mass flow rates by the effect of mesh, working fluid, fins and geometry of the FHPHE. This significance of results are analysed for the Effectiveness, Reynolds number, Heat transfer coefficient and Heat transfer rate. The copper fins act as extended surfaces that increase the effective area for convective heat transfer between the condenser and cold fluid. They reduce the overall thermal resistance by lowering the convection resistance. They enhance the rate of condensation on the condenser wall by improving heat removal, thus sustaining the evaporation–condensation cycle inside the pipe. They increase turbulence in the cold-side flow, reducing boundary layer thickness and enhancing the convective heat transfer coefficient. This synergistic effect ensures that more vapor can condense per unit time, raising the system's heat transfer coefficient and overall effectiveness.

The investigation is carried out initially with hot fluid inlet temperature of  $70^\circ\text{C}$ ,  $m_{hi}$  of 0.0138 kg/s and  $m_{ci}$  as 0.069 kg/s with  $33^\circ\text{C}$  as ambient cold fluid temperature throughout the experimentation, the obtained result shows that 17.6% as effectiveness is given in the Figure 6 and equation (1), (2). The experimentation is conducted for different  $m_{hi}$  such as 0.0277, 0.0416 and 0.0555 kg/s, and similarly for  $m_{ci}$  as 0.0139, 0.0208 and 0.0278 kg/s. The investigation shows that for same temperature of  $70^\circ\text{C}$ , at 0.0555 kg/s the observed effectiveness is 29.3%. The investigation is further carried out for different input temperatures of  $75^\circ\text{C}$ ,  $80^\circ\text{C}$ ,  $85^\circ\text{C}$  and  $90^\circ\text{C}$ . Studies results for 0.0555 and 0.0278 kg/s for the different input temperature the values are 30.5%, 35.7%, 38.09% and 39.1%. This shows that at  $T_{hi}$  as  $90^\circ\text{C}$ ,  $m_{hi}$  as 0.0555 kg/s and  $m_{ci}$  as 0.0278 kg/s shows highest effectiveness of the system of 39.1%. The results clearly shows that while comparing the  $m_{hi}$  from 0.0138 to 0.0555 kg/s at  $70^\circ\text{C}$  there is the improvement of 66.4%, this shows that at 0.0555 kg/s the maximum results are observed, hence for the same 0.0555 kg/s while comparing the effectiveness from  $70^\circ\text{C}$  to  $90^\circ\text{C}$  there is improvement in results of 33.4%. The entry and exit of cold fluid temperatures

are given by  $T_{c,o}$  and  $T_{c,i}$ , similarly for  $T_w$ ,  $T_b$ ,  $T_s$  states the temperatures of wall, bulk mean and surface, respectively.

The T-shaped HP using fins along the condenser section makes maximum heat transfer. This is occurred due to the influence of the wick induce the capillary action inside the heat pipe thus vapour formation and movement occurs gradually and the influence of the DI water makes reportable improvement in the heat transfer performance based on the geometry of the HP, this makes enhanced temperature difference in the condenser section leads to the higher heat transfer performance. The influence of the maximum mass flow rate leads to the increased effectiveness due to the maximum liquid contact between the heat pipes, makes the quick vapour formation to the working fluid leads to the higher effectiveness on FHPHE. The equation of FHPHE for effectiveness is given by,

$$\text{Effectiveness } (\epsilon) = \frac{Q_{actual}}{Q_{max\ possible}} \quad (1)$$

$$\epsilon = \frac{T_{c,o} - T_{c,i}}{T_{h,i} - T_{c,i}} \quad (2)$$

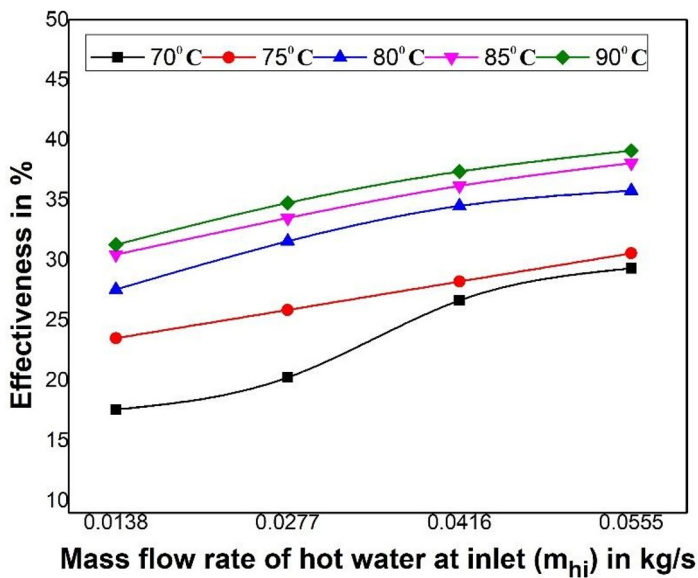


**Fig 6.** Influence of Mass flow rate on Effectiveness

The experimentation is conducted for heat transfer coefficient and mass flow rate shown in Figure 7. The analysis is done for initial  $T_{hi}$  of 70°C,  $T_{ci}$  as 33 °C,  $m_{hi}$  as 0.0138 kg/s, and  $m_{ci}$  as 0.069 kg/s results in heat transfer coefficient ( $h$ ) as 188.40 W/m<sup>2</sup>°C. Experimentation is conducted for different  $m_{hi}$  such as 0.0277, 0.0416 and 0.0555 kg/s, and similarly for  $m_{ci}$  as 0.0139, 0.0208 and 0.0278 kg/s using the equation (3). The investigation shows that for same

temperature of 70°C, at 0.0555 kg/s the observed (h) is 1442.68 W/m<sup>2</sup>°C. The investigation is further carried out for different input temperatures of 75 to 90°C. Results calculated for 0.0555 and 0.0278 kg/s for the different input temperature the values are 1813.07, 1906.39, 2116.91, and 2211.91 W/m<sup>2</sup>°C. This shows that at T<sub>hi</sub> as 90°C, m<sub>hi</sub> as 0.0555 kg/s and m<sub>ci</sub> as 0.0278 kg/s shows highest (h) of the FHPHE is 2211.91 W/m<sup>2</sup>°C.

$$h_c = \frac{\dot{m}_c c_{pc} (T_{c,o} - T_{c,i})}{A_c (T_w - T_b)} \tag{3}$$

The influence of the DI water forms the vapour and due to the wire mesh in the FHPHE the capillary action of wick makes the quick phase transformation along evaporator to condenser zone. This induces the maximum heat transfer coefficient in the system. The vertical orientation of the heat pipe makes the vapour movement along the HP with the capillary action of wick also makes the fast heat transfer in the FHPHE, by comparing the m<sub>hi</sub> from 0.0138 to 0.0555 kg/s at 70°C shows improvement in (h) of 665%, this shows that at 0.0555 kg/s the maximum results are observed, hence for this 0.0555 kg/s while comparing the (h) from 70°C to 90°C there is improvement in results of 53%.

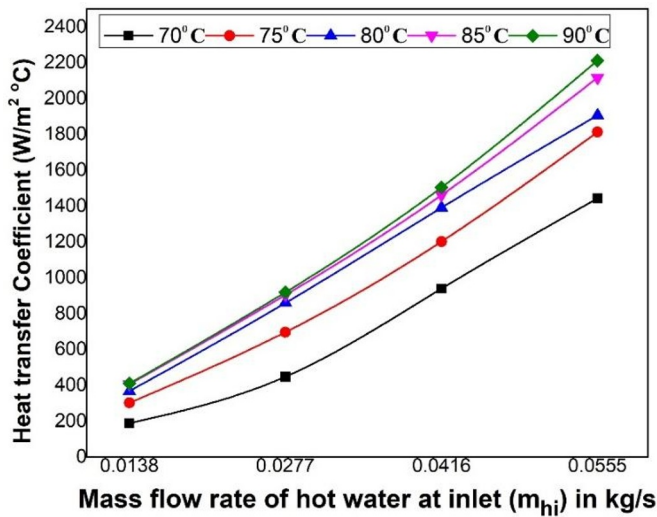


**Fig 7.** Influence of Mass flow rate on Heat transfer coefficient

The analysis is carried out for heat transfer rate (Q) and mass flow rate (m<sub>hi</sub>) is given in Figure 8 and equation (4). The study focus on the influence of DI water in FHPHE makes the improvement in heat transfer for different temperature and mass flow rates, this enhancement is achieved by uniform heat transfer inside the system. The results are observed at T<sub>hi</sub> of 70°C, T<sub>ci</sub> as 33 °C, m<sub>hi</sub> as 0.0138 kg/s, and m<sub>ci</sub> as 0.069 kg/s possess the heat transfer rate (Q) of 191.85 W. The experimentation is conducted for different m<sub>hi</sub> such as 0.0277, 0.0416 and 0.0555 kg/s, and similarly for m<sub>ci</sub> as 0.0139, 0.0208 and 0.0278 kg/s. The investigation shows that for same temperature of 70°C, at 0.0555 kg/s the observed (Q) is 1279.05 W. The investigation is further carried out for different input temperatures of 75°C to 90°C. The results obtained for 0.0555 and 0.0278 kg/s for the different input temperature the values are 1511.61

W, 1976.72 W, 2325.55 W, and 2616.25 W. This shows that at  $T_{hi}$  as  $90^{\circ}\text{C}$ ,  $m_{hi}$  as  $0.0555 \text{ kg/s}$  and  $m_{ci}$  as  $0.0278 \text{ kg/s}$  shows highest (Q) of the system of 2616.25 W. The  $m_{hi}$  from  $0.0138$  to  $0.0555 \text{ kg/s}$  at  $70^{\circ}\text{C}$  there is the improvement in (Q) of 566%, this shows that at  $0.0555 \text{ kg/s}$  the maximum results are observed, hence for this  $0.0555 \text{ kg/s}$  while comparing the (Q) from  $70^{\circ}\text{C}$  to  $90^{\circ}\text{C}$  there is improvement in results of 104%. This is 104 % increment in Q while relating with different  $m_{hi}$  at DI water makes the significant increment trend is obtained because of the impact of wick induces the capillary action on HP thus the circulation of WF as higher grade energy source from evaporator toward condenser and subsequently condensing the lower grade energy returns to evaporator. This phenomena occurs in HP because of the capillary action and pressure variance. The results are attained because of the occurrences that, maximum integration of thermal energy to water by the liquid WF and hence, phase change happens. It leads to the energy transfer happens in working fluid, likewise when relating DI water has higher heat transfer rate. The Fins in the HP makes the contact between cold fluid and HP surface this makes the higher heat transfer in the condenser section.

$$Q_c = \dot{m}_c c_{pc} (T_{c,o} - T_{c,i}) \quad (4)$$

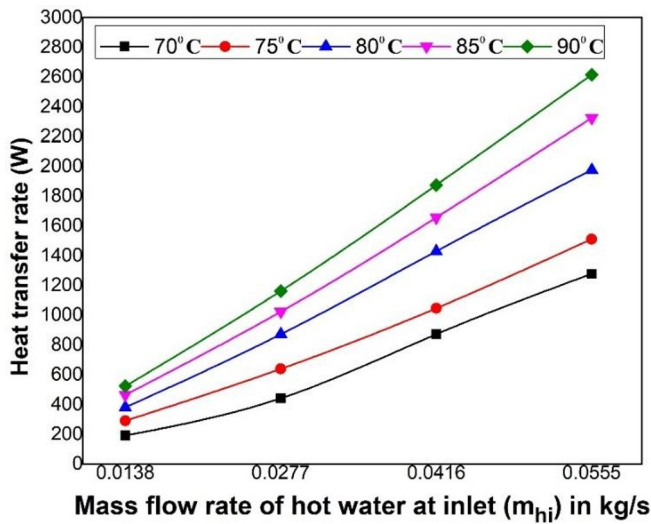


**Fig 8.** Influence of Mass flow rate on Heat transfer rate

This study focus on the Reynolds number (Re) on mass flow rate ( $m_{hi}$ ) is given in Figure 9. The investigation is carried out with the effect of DI water in HP possess the enhancement in performance for different temperature and mass flow rates, this enhancement is achieved by uniform heat transfer inside the system. The results are observed at  $T_{hi}$  of  $70^{\circ}\text{C}$ ,  $T_{ci}$  as  $33^{\circ}\text{C}$ ,  $m_{hi}$  as  $0.0138 \text{ kg/s}$ , and  $m_{ci}$  as  $0.069 \text{ kg/s}$  gives the (Re) of 542. The experimentation is conducted for different  $m_{hi}$  such as  $0.0277$ ,  $0.0416$  and  $0.0555 \text{ kg/s}$ , and similarly for  $m_{ci}$  as  $0.0139$ ,  $0.0208$  and  $0.0278 \text{ kg/s}$ . The investigation shows that for same temperature of  $70^{\circ}\text{C}$ , at  $0.0555 \text{ kg/s}$  the observed (Re) is 2171. This shows that at less (Re) the viscous force ruled the inertia force which leads to the minimum results. The investigation is further carried out for different input temperatures of  $75^{\circ}\text{C}$  to  $90^{\circ}\text{C}$ . The results obtained for  $0.0555$  and  $0.0278 \text{ kg/s}$  for the different

input temperature the values are 2195, 2211, 2456 and 2771, this phenomena is achieved by enlarging the fluid flow rate, the inertia force overwhelms the viscous forces hence, it shows the increase in Re which leads to an increase in thermal efficiency.

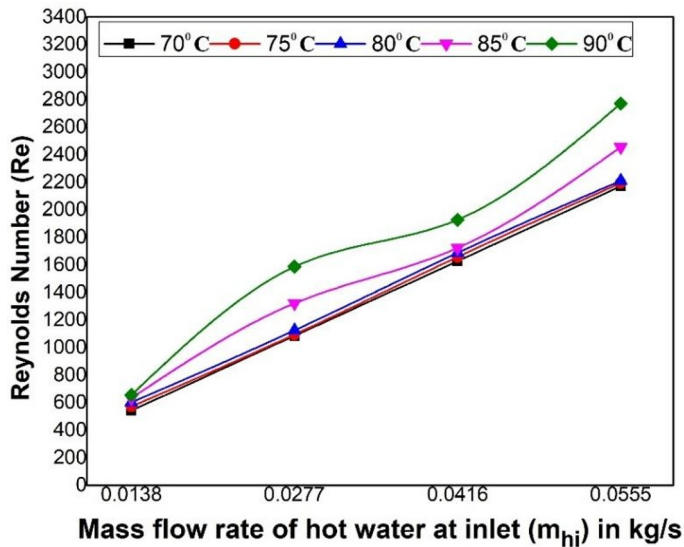


**Fig 9.** Influence of Mass flow rate on Reynolds number

This shows that at  $T_{hi}$  as  $90^{\circ}\text{C}$ ,  $m_{hi}$  as  $0.0555$  kg/s and  $m_{ci}$  as  $0.0278$  kg/s shows highest Reynolds number of the system of 2771. The  $m_{hi}$  along  $0.0138$  to  $0.0555$  kg/s at  $70^{\circ}\text{C}$  there is the improvement in (Re) of 300%, this shows that at  $0.0555$  kg/s the maximum results are observed, hence for this  $0.0555$  kg/s while comparing the (Q) from  $70^{\circ}\text{C}$  to  $90^{\circ}\text{C}$  there is improvement in results of 27%. This is known that, the Re is the function of inertia and viscous forces using the equation (5). At low flow rates (Re - 542), viscous forces dominate, resulting in weaker convection and lower heat transfer. At higher flow rates (Re - 2771), inertia becomes dominant, thinning the thermal boundary layer and enhancing convection. However, since  $Re < 2300$  typically indicates laminar flow, these results suggest the system was in a laminar transition regime. Despite laminar flow, the presence of fins and phase-change dynamics created effective turbulence at the micro-scale, ensuring uniform and enhanced heat transfer. Thus, the Reynolds number not only characterizes the flow regime but also shows how finned heat pipe geometry can overcome laminar limitations to achieve high heat transfer coefficients.

The Reynold's number of the experimentation is calculated,

$$Re = \frac{4\dot{m}_c}{\pi D_c \mu} \tag{5}$$

The DI water in finned heat pipe makes the highest heat transfer, at maximum mass flow rate and temperature due to this Re will gets increased. Even though the flows makes higher heat

transfer and fins makes maximum contact between fluid and heat pipe the observed Reynolds number shows flow in laminar condition.

## 4 Conclusion

In this investigation the finned heat pipe is designed and analysed in the compact heat exchanger with DI water as working fluid using different heat input temperature and mass flow rates. The analysis reveals that at  $T_{hi}$  of 90°C,  $T_{ci}$  of 33°C,  $m_{hi}$  of 0.0555 kg/s, and  $m_{ci}$  as 0.0278 kg/s the maximum performance and optimum condition in the system. The effectiveness of the system for the optimum condition reveals 39.1% and similarly for minimum  $T_{hi}$  of 70°C at same mass flow rates observes 29.3% this shows improvement in effectiveness of 33.4%. The heat transfer coefficient for optimum condition possess 2211.91 W/m<sup>2</sup>°C, for the same mass flow rates at  $T_{hi}$  of 70°C the observed (h) is 1442.68 W/m<sup>2</sup>°C this gives increment in the results of 53%. The influence of heat transfer rate on the optimum condition predicts 2616.25 W, for similar mass flow rate and for 70°C temperature the Q is 1279.05 W, this shows enhanced results of 104%. The Reynolds number of this system shows for similar condition as 2771, and for  $T_{hi}$  of 70°C for same mass flow rates it calculates 2171, this Re shows the increment in results of 27%. The higher heat transfer is observed for Re of 2771 the flow is laminar throughout the experimentation, thus flow is uniform and regular in pattern. This experimentation shows that at optimum condition the results observed are higher for this FHPHE set up. The setup can be used for the utilization of the waste heat from the exhaust and it is utilised as the useful heat for the required application in industries as waste heat recovery system.

## References

1. J. Kassim and H. Hashim, Experimental and mathematical research of convection heat transfer for a high integral finned tube heat exchanger. *J. Eng. Sustain. Dev.* 23(6), 70–83 (2019). <https://doi.org/10.22124/jesd.2019.14087>
2. M. S. Kassim and H. S. Gaber, Investigation of convection heat transfer for high integral finned tube heat exchanger. (2020). DOI unavailable.
3. D. Luo, S. Yang, Y. Yan, J. Cao, and B. Y. Cao, Performance improvement of the automotive thermoelectric generator by extending the hot side area of the heat exchanger through heat pipes. *Energy Rep.* (2021). <https://doi.org/10.1016/j.egy.2021.02.008>
4. X. Liu and Y. Chen, Transient thermal performance analysis of micro heat pipe. *Int. J. Heat Mass Transf.* 123, 456–467 (2018). <https://doi.org/10.1016/j.ijheatmasstransfer.2018.03.041>
5. R. W. MacGregor, P. A. Kew, and D. A. Reay, Investigation of low global heating potential working fluids for a closed two-phase thermosiphon. *Appl. Therm. Eng.* 175, 115338 (2020). <https://doi.org/10.1016/j.applthermaleng.2020.115338>
6. M. Mameli, L. Araneo, S. Filippeschi, L. Marelli, R. Testa, and M. Marengo, Thermal response of a closed loop pulsating heat pipe under a varying gravity force. *Int. J. Therm. Sci.* 139, 108–119 (2019). <https://doi.org/10.1016/j.ijthermalsci.2019.04.017>
7. M. Miscevic, G. El Achkar, P. Lavieille, A. Kaled, and S. Dutour, About flow regime and heat transfer in low diameter condenser of LHP and CPL. *Heat Mass Transf.* 57, 2345–2355 (2021). <https://doi.org/10.1007/s00231-021-02955-5>

8. D. Mishkinis, P. Prado, R. Sanz, and A. Torres, Development of LHP for intermediate temperature range. *Appl. Therm. Eng.* 178, 115462 (2020). <https://doi.org/10.1016/j.applthermaleng.2020.115462>
9. L. Mottet, T. Coquard, and M. Prat, Three-dimensional liquid and vapor distribution in the wick of capillary evaporators. *Int. J. Heat Mass Transf.* 118, 35–46 (2018). <https://doi.org/10.1016/j.ijheatmasstransfer.2017.11.080>
10. V. S. Nikolayev, Dynamics of the triple contact line on a non-isothermal heater at partial wetting. *J. Colloid Interface Sci.* 487, 302–314 (2017). <https://doi.org/10.1016/j.jcis.2016.11.070>
11. V. S. Nikolayev, A dynamic film model of the pulsating heat pipe. *Int. J. Heat Mass Transf.* 135, 736–748 (2019). <https://doi.org/10.1016/j.ijheatmasstransfer.2019.01.016>
12. M. Nishikawara, H. Nagano, and T. Kaya, Transient thermo-fluid modeling of loop heat pipe and experimental validation. *Appl. Therm. Eng.* 188, 116611 (2021). <https://doi.org/10.1016/j.applthermaleng.2021.116611>
13. N. Kim and S. Kim, Self-convectonal three-dimensional integrated circuit cooling system using micro flat heat pipe for portable devices. *Microelectron. J.* 96, 51–61 (2020). <https://doi.org/10.1016/j.mejo.2020.104899>
14. E. W. Washburn, *International Critical Tables of Numerical Data, Physics, Chemistry and Technology*. National Research Council, The National Academies Press, Washington, D.C. (1930).
15. J. P. Holman, *Experimental Methods for Engineers*, 7th ed. McGraw-Hill, New York (2007).